Clays and Clay Minerals, Vol. 69, No. 3:354–365, 2021

STACKING DISORDER AND REACTIVITY OF KAOLINITES

Bidemi Fashina and Youjun Deng*
[1]Department of Soil and Crop Sciences, Texas A&M University, College Station, TX 77843-2474, USA

Abstract—Kaolinite is a clay mineral with diverse environmental, industrial, and agricultural applications. The influence of the crystallographic properties of kaolinite, e.g. structural disorder, on these applications is of great interest. Qualitative and quantitative analyses of kaolinite structural disordering over the last 70 years have revealed three main sources of layer-stacking disordering: (1) enantiomorphic stacking; (2) dickite-like stacking; and (3) random shift of layers. What influence do these stacking disorders have on the reactivity of kaolinite? The objective of the present study was to investigate the influence of stacking disorder on the intercalation and dissolution of kaolinite layers. To minimize the effect of particle size on reactivity, the 1–2 μm fractions of five geologic kaolinites were used. The 1–2 μm fractions varied in the degree of structural disorder. The kaolinites were: (1) intercalated with saturated CH_3COOK solution at room temperature to examine the effect of stacking disorder on intercalation; and (2) dissolved in 4 M NaOH at 80°C to examine the effect of stacking disorder on kaolinite stability in alkaline solution. Samples with a low degree of stacking disorder intercalated twice as much and dissolved >1.5 times as much as the most disordered sample. The infrared spectrum of the undissolved kaolinite residue in 4 M NaOH showed relative intensities of OH-stretching bands characteristic of a kaolinite-dickite mixture. The binding strength (i.e. resistance to intercalation) of the undissolved residue by NaOH was high; the residue could not be intercalated by CH_3COOK. Differences in the average interlayer binding strength were attributed to the greater proportions of dickite-like sequences in highly disordered kaolinite compared to ordered kaolinite specimens. These results suggested that the binding strength of kaolinite layers is proportional to the degree of stacking disorder. Dickite-like sequences, a type of stacking defect, contributed to the lower reactivity of highly disordered kaolinite.

Keywords—Dissolution · Intercalation · Interlayer binding strength · Kaolinite · Structural disorder

INTRODUCTION

Kaolinite is a 1:1 dioctahedral member of the kaolin subgroup of minerals with an ideal formula of $Al_2Si_2O_5(OH)_4$. Each 1:1 layer consists of a silica tetrahedral sheet and a dioctahedral alumina octahedral sheet (Fig. 1). Successive layers are held together primarily by long hydrogen bonds along the *c* axis (Giese, 1973). Two of the three (A, B, and C) possible octahedral sites in the octahedral sheet are occupied by Al. The layers are designated A, B, or C depending on the position of the unoccupied octahedral site (Fig. 2).

Structural disorder in kaolinite could either be natural — through crystal growth, polymorphic transformations (Veblen, 1985), transport processes (White & Dixon, 2002) — or mechanically induced through milling (Kristof et al., 1993), sonication (Franco et al., 2003), etc. An ideal, perfect (defect-free) kaolinite has stacks of only one layer type (CC… stacking sequences) with a layer displacement vector $\mathbf{t_1}$ (≈ $-a/3$) or $\mathbf{t_2}$ (≈ $a/6–b/6$). The relationship between $\mathbf{t_1}$ and $\mathbf{t_2}$ is a pseudo-mirror plane passing through the center of the vacant octahedral site of the kaolinite unit cell (Bookin et al., 1989; Drits & Tchoubar, 1990; Giese, 1988). This pseudo-mirror reflection makes the $\mathbf{t_1}$ and $\mathbf{t_2}$ displacements symmetric about the pseudo-mirror plane. Herein, the layers in a $\mathbf{t_2}$ displacement are denoted as C^eC^e. Most stacking disorder in kaolinite is introduced into the structure by random interstratification of $\mathbf{t_1}$ and $\mathbf{t_2}$ displacement vectors (Bookin et al., 1989; Plançon et al., 1989). Results from high-resolution transmission electron microscopy (HRTEM) studies and the modeling of X-ray diffraction (XRD) patterns have revealed that the interstratification of enantiomorphic C layers (i.e. CC^e) is the most common source of stacking disorder in kaolinite (Plançon et al., 1989; Kogure et al., 2010; Kogure, 2011; Sakharov et al., 2016). Though present in just small proportions, another form of stacking disorder that has been observed in kaolinites arises from the alternation of C and B (±120° mutual rotation between adjacent layers in ideal structures) layers (Plançon et al., 1989; Kogure et al., 2010; Kogure, 2011). The regular CB… or BC… stacking sequence with the $\mathbf{t_1}$ displacement is characteristic of dickite — another member of the kaolin subgroup of minerals. Dickite-like sequences in kaolinite have been confirmed in HRTEM studies (Kogure et al., 2010; Kogure, 2011). Infrared spectra of some kaolinites have shown dickite-like features, such as enhanced 3650 and 3620 cm^{-1} bands, suggesting that the random stacking of kaolinite and dickite-like layers is one of the sources of disorder in kaolinites (Beauvais & Bertaux, 2002; Fraser et al., 2002; Johnston et al., 2008; Prost et al., 1989). Another form of minor stacking disorder is due to the layer displacement $\mathbf{t_0}$ (≈ $-0.3154a – 0.3154b$), located along the long diagonal of the oblique layer unit cell that contains the vacant octahedral site (Sakharov et al., 2016). To model the XRD patterns of kaolinites successfully, it was necessary to incorporate some dickite-like sequences or displacement vectors ($\mathbf{t_o}$) that have similar effects to introducing B layers (Bookin et al., 1989; Plançon et al., 1989; Sakharov et al., 2016).

Because it is the most common type of disorder in clays (Brindley, 1980; Lombardi et al., 1987), stacking disorder in kaolinites has been studied extensively during the past ~70 years using both qualitative and quantitative approaches.

* E-mail address of corresponding author: yjd@tamu.edu
DOI: 10.1007/s42860-021-00132-x

© The Clay Minerals Society 2021

https://doi.org/10.1007/s42860-021-00132-x Published online by Cambridge University Press

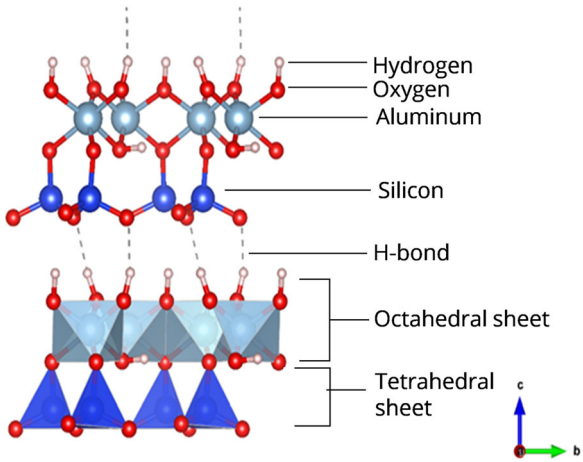


Fig. 1. Ball and stick (upper) and polyhedral (lower) representation of the kaolinite structure

Given that the properties of minerals are a function of chemical and structural blueprints, addressing the implications of order-disorder for the reactivities and applications of kaolinites is critical, but many contrary observations have been reported in the literature.

Structural Disorder and Reactivity of Kaolinites

Few studies have attempted to address the question above by investigating the influence of stacking disorder in kaolinites on the properties: rate and degree of intercalation, rate of dissolution and transformation, and thermal stability.

Intercalation of kaolinites by organic molecules is important for producing nanoparticles for desired agricultural, environmental, and industrial applications (Sugahara et al., 1991; Mahdavi et al., 2014). The ease and extent of intercalation determines the quantity and quality of the nanoparticles recovered as well as their applications. Conclusions drawn about the effect of stacking disorder on the intercalation of kaolinite are often non-definitive or contradictory. In some studies, highly ordered layers were easier to intercalate (Frost et al., 1999; Deng et al., 2002; Cheng et al., 2010) which suggests a weaker interlayer binding strength, in a domain with the same type of stacking sequence, than that between two domains with different stacking sequences. Others have recorded an opposite trend (Wiewióra & Brindley, 1969; Cruz-Cumplido et al., 1982) or concluded that the interlayer binding strength of kaolinite layers was not influenced by structural disorder (Uwins et al., 1991, 1993).

The dissolution and transformation of kaolinite, particularly in alkaline solution, has long been studied. The dissolution of kaolinite in alkaline solution at elevated temperature is a fast process and is used as a source of Al and Si for the synthesis of a variety of geopolymers, zeolites, and feldspathoids (Panagiotopoulou et al., 2007; Reyes et al., 2013; Xu et al., 2010; Zhao et al., 2004). The extent of kaolinite dissolution determines the quantity of Al and Si in solution and determines indirectly the properties and applications of the synthesized materials. An experiment lasting for up to 4 weeks concluded that structural disorder did not influence the transformation of kaolinite to sodalite in NaOH (Zhao et al., 2004). In another study, highly disordered kaolinite dissolved twice as quickly as highly ordered kaolinite in oxalic acid but a similar dissolution rate was observed in HNO_3 (Sutheimer et al., 1999). The latter authors suggested that "the fundamental structure of kaolinite, rather than specific surface details, exerts the greatest influence on dissolution kinetics." A study of the slow dissolution of seven kaolinites, in pH 3 0.001 N HCl for 2 months, indicated that highly disordered samples dissolved more quickly than low disordered kaolinites (Kittrick, 1966; Devidal et al., 1996).

Results from the energy-of-formation experiments determined from drop-solution calorimetry for four kaolinites suggested that structural disorder did not influence the stability of kaolinite layers (De Ligny & Navrotsky, 1999). A solubility approach found that the energy of formation increased slightly (–903.8 to –902.5 kcal/mol) as structural disorder increased (Kittrick, 1966).

The dehydroxylation temperature of kaolinite decreased as structural order decreased (Stoch & Wacławska, 1981; Bellotto et al., 1995; Vaculikova et al., 2011) but the activation energy (E_a) increased in the same direction (Horváth, 1985; Vaculikova et al., 2011). By heating two kaolinite samples at different heating rates, E_a was derived to be 40(6) kcal/mole for highly ordered KGa-1 and 22(7) kcal/mole for low-ordered kaolinite KGa-2, respectively (Bellotto et al., 1995). The calculated activation energies by the latter authors were more plausible as they made no assumption about the kinetic equation.

In summary, no consensus seems to exist on the influence of structural disorder on the reactivity of kaolinites. Two reasons for the contradictory observations/conclusions may stem from: (1) the use of the Hinckley index (HI) as a measure of the extent of structural disorder in kaolinites; and (2) particle-size variations amongst samples in addition to their disordering differences. In studies targeted at investigating the relationship between structural disorder and reactivity/stability of kaolinite layers, the commonly used parameter in estimating the extent of structural disorder is the HI (Hinckley, 1962) or similar empirical parameters such as the Lietard (R2) index (Liétard, 1977) or the Aparicio-Gálan-Ferrell index (Galán et al., 2006). These indices estimate the abundance of structural disorder in kaolinite as a "crystallinity index" by calculating ratios of the intensities (after subtracting background) of XRD peaks (020, 110, and $11\bar{1}$ reflections) between 19 and 26°2θ (CuKα radiation). Kaolinites, the XRD patterns of which are characterized by well resolved peaks and low background between 19 and 26°2θ (CuKα radiation), usually have high HI values and are considered less structurally disordered than specimens with high background and poorly resolved peaks. Given that the observed shape of the XRD reflection is a convolution

https://doi.org/10.1007/s42860-021-00132-x Published online by Cambridge University Press

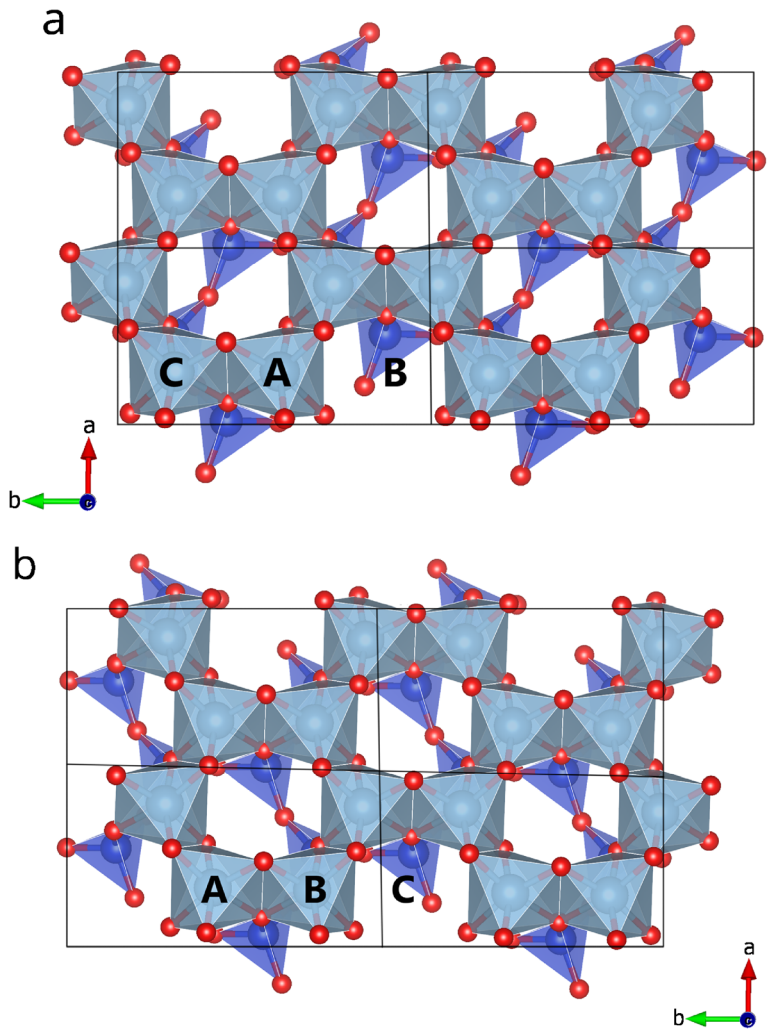


Fig. 2. 2×2×1 (*x*,*y*,*z*) kaolinite layer types: **a** B and **b** C with vacant B and C positions, respectively. Based on atomic coordinates by Bish and Von Dreele (1989)

of both instrumental and sample contributions, kaolinite specimens consisting of small crystallites/particle size have broader (less resolved) XRD peaks compared to specimens with larger particle size. Consequently, this yields a lower HI value in the former even if both specimens have the same extent of structural disorder within the assemblages. For this reason, the use of HI as an estimate to compare structural disorder amongst kaolinites should be done with an awareness of the influence of 'size' on measured HI values. To avoid or minimize this bias, it is imperative that the specimens being compared have a similar mean distribution of particle size. Unfortunately, the influence of size is seldom considered when comparing HI values amongst kaolinite specimens. Huge variations in the distribution of particle sizes also influence the observed reactivity or stability (Deng et al., 2002; Horváth, 1985). For example, it is generally accepted that intercalation in kaolinites becomes more difficult as the particle size decreases (Deng et al., 2002; Uwins et al., 1993). Hence, samples containing most particles within the fine fraction might intercalate more slowly and to a lesser extent than samples with larger particles irrespective of the degree of disorder in either sample (Uwins et al., 1993).

The influence of stacking disorder on the reactivity of kaolinites remains unclear. Given the variations (translations, type of layers, etc.) in the stacking of disordered/ordered kaolinite layers, the hypothesis is that structural disorder will influence the reactivity of kaolinites. The objective of the present study was, therefore, to investigate the influence of stacking disorder on the intercalation and dissolution of kaolinite layers.

MATERIALS AND METHODS

Sample Preparation and Preliminary Analysis

Five geologic kaolinite specimens were collected from Georgia, USA, and coded as Kao-01, -02, -03, -05, and

https://doi.org/10.1007/s42860-021-00132-x Published online by Cambridge University Press

-Huber. The Huber sample was supplied by the J.M. Huber Corporation; the others were collected during the field trip of the 53rd Annual Meeting of The Clay Minerals Society in Georgia. All samples were air-dried, crushed in a mortar, and passed through a 2-mm sieve. Samples were treated with pH 5 sodium acetate buffer solution, 30% hydrogen peroxide, and dithionite-citrate-bicarbonate to remove carbonate minerals, organic matter, and iron oxides, respectively. To constrain the influence of particle size on HI values and reactivity, the 1–2 μm fraction of each sample was separated from the bulk by centrifugation (Soukup et al., 2008).

The extent of structural disorder in the samples was estimated from the XRD patterns by the Hinckley method, and crystallite size by Scherrer's equation, respectively (Scherrer, 1918; Hinckley, 1962). Dispersion of each of the 1–2 μm samples in water was used to estimate the particle-size distribution using a laser diffraction particle size analyzer (LS230, Beckman Coulter). The morphology and chemical composition of the kaolinite samples were studied using an FEI Quanta 600F field emission scanning electron microscope (SEM) equipped with X-ray energy dispersive spectroscopy (EDS) (FEI, Hillsboro, Oregon, USA). The XRD patterns were recorded on a Bruker D8 ADVANCE X-ray diffractometer (Bruker AXS GmbH, Karlsruhe, Germany) with CuKα radiation operated at 40 kV and 40 mA. A programmable divergent slit, with a constant 12 mm radiation length and a Sol X detector was used for the XRD analysis. Powdered samples were front-loaded on a sample holder and patterns were recorded in the range 5–70°2θ, with a step size of 0.02°2θ and a dwell time of 3 s at each step. Kaolinite and accessory minerals in the samples were quantified by Rietveld refinement (Rietveld, 1967). Structural models were visualized using VESTA (Momma & Izumi, 2011).

Kaolinite Intercalation Experiment

An amount of 0.1 g of clay was dispersed in 5 mL of deionized (DI) water followed by transfer of 200 μL of the dispersion onto pre-weighed (W_1) glass disks. The dispersions on the disks were left to air dry at room temperature for 24 h after which the mass of the glass and clay film was determined (W_2). The difference between W_1 and W_2 is the mass of clay on each glass disk. Two drops of saturated potassium acetate (CH_3COOK) solution were pipetted onto the air-dried clay film and the mass recorded immediately (W_3). The glass disk was immediately transferred to the XRD instrument and patterns were acquired subsequently in situ between 0 and 120 h to monitor the rate and degree of intercalation of the clays. The difference between W_3 and W_2 is the mass of saturated CH_3COOK solution on each clay film. The mass of clay was ~4 mg while the mass of CH_3COOK solution was ~70 mg. The XRD patterns were recorded between 2 and 32°2θ, with a step size of 0.05°2θ and a dwell time of 3 s at each step.

When CH_3COOK molecules intercalate kaolinite, the interlayer distance expands from 7 Å (kaolinite) to ~14 Å (kaolinite-CH_3COOK complex). The proportion of the interlayer penetrated by the molecules was estimated as (Theng, 1974):

$$\%\text{Intercalation} = \frac{I_{\text{kao–CH3COOK}}}{I_{\text{kao}} + I_{\text{kao–CH3COOK}}} X100\% \quad (1)$$

where I_{kao} and $I_{kao\text{-}CH3COOK}$ are the intensities of the 7 and 14 Å reflections, respectively.

Kaolinite Dissolution and Transformation in 4 M NaOH

Only three of the kaolinite specimens, Kao-01, 03, and 05, with large HI differences, were used in the NaOH dissolution experiment. These samples represented the least disordered, medium disordered, and the most disordered, respectively, of the five samples considered. The dissolution experiment was conducted by mixing 0.1 g of each kaolinite sample with 8 mL of 4 M NaOH solution and 2 mL of 0.5 M NaCl in 15-mL polypropylene centrifuge tubes. The tubes were capped and kept in the oven at 80°C for 3 days and were agitated by hand every 12 h.

By the end of the experiment, to halt further dissolution, the tubes were immediately filled to 15 mL with DI water, centrifuged, and the supernatant discarded. The residue was washed twice more with DI water to rid the residue of alkali solution. The residues were then left to air dry on glass disks for 24 h before further analysis.

Infrared (IR) spectra of the three samples before and after dissolution by NaOH were recorded as an average of 32 scans at 4 cm^{-1} resolution using a Perkin Elmer Spectrum 100 Fourier-transform infrared spectrometer (FTIR) (Perkin Elmer, Waltham, Massachusetts, USA) equipped with a 45° single reflection diamond crystal universal attenuated total reflection (ATR) accessory. The residues, after dissolution, were also analyzed by XRD (on glass disks).

At the end of the NaOH dissolution experiment, the intensity of the XRD and IR peaks of kaolinite was expected to diminish or disappear completely while new peaks from sodalite emerged. Residual kaolinite was estimated by Rietveld refinement and the percent dissolution was calculated as shown below:

$$\%\text{Dissolution} = \frac{Q_{k(s)} - Q_{k(d)}}{Q_{k(s)}} X100\% \quad (2)$$

where $Q_{k(s)}$ and $Q_{k(d)}$ are the proportions of kaolinite in the starting material and the quantity after dissolution in NaOH, respectively. Using anatase (accessory mineral) as an indirect internal standard, given its stability under the experimental conditions, the amorphous content can be estimated and not assigned as clay. Orientation preference was expected to occur on the disks for residual kaolinite from the NaOH dissolution experiment. The small amounts of the starting kaolinite in the NaOH dissolution experiment would increase the error of the Rietveld quantification. The intensities of the OH bands of the residual kaolinites were also compared with calculated $Q_{k(d)}$ to check if they followed the same trend.

https://doi.org/10.1007/s42860-021-00132-x Published online by Cambridge University Press

Extraction and Purification of the Less-reactive Kaolinite Phase in the NaOH Dissolution Experiment

One of the sodalite-kaolinite residues was selected to study further the residual kaolinite that was not dissolved during the 72-h NaOH dissolution experiment. The sodalite-kaolinite residues from the dissolution of kao-01 were chosen because the amount of residual kaolinite was adequate and mica was absent, as in kao-5. The residue was washed in 1 M HCl for 30 min followed by twice washing in DI water and centrifugation. The HCl washing was used to dissolve sodalite and amorphous phases while the DI washing rid the matrix of the dissolved Al and Si. The resulting residue corresponded to the kaolinite phase that was less reactive to NaOH dissolution. SEM images and an FTIR spectrum of the less-reactive residue were acquired. The intercalation experiment was repeated on the 'less reactive' kaolinite phase to investigate the binding strength of the layers.

RESULTS

Kaolinite Sample Properties

From the XRD patterns of the 1–2 μm fraction of the five kaolinites (Fig. 3), the extent of structural disorder followed the trend: kao-05 > kao-huber > kao-02 > kao-01 > kao-03. The less disordered samples had well resolved peaks and a low background of between 4.46 and 3.58 Å compared to the highly disordered samples. The kaolinite content in all the samples was >95% and the crystallite size (00*l*) ranged from 41 to 71 nm based on XRD peak fitting (Table 1). All the samples had a similar chemistry (Fig. 4a), similar particle-size distribution (Fig. 4b), and contained a small amount of accessory minerals (anatase and mica) (Table 1, Fig. 3). These analyses indicated that the particle size and chemistry of the samples could be regarded as similar and should have similar effects on the reactivities in the intercalation and dissolution in this study.

Effect of Disordering in Kaolinite on the Rate of Intercalation by CH_3COOK

As intercalation progressed, the kaolinite 7.16 Å reflection decreased in intensity while the reflection at ~14 Å of the kaolinite-CH_3COOK became more intense (Fig. 5a). The latter peak was due to the increase in the interlayer spacing as the CH_3COOK molecules accrued in the interlayer of kaolinite. In the first 6 h of the intercalation experiment, the samples with a low degree of structural disorder intercalated more quickly than samples with a higher degree of disorder; the most ordered sample (kao-03) intercalated twice as much as the most disordered (kao-05) sample (Fig. 5b). By the end of the experiment, samples with the lowest extent of disordering recorded the greatest degree of intercalation (Fig. 5b).

Effect of Disordering on the Kaolinite Dissolution and Transformation in NaOH Solution — XRD and FTIR Data

The majority of kaolinite in all of the specimens was dissolved in the 4 M NaOH solution under current experimental conditions, but small differences in the percentages of residual kaolinite was difficult to quantify accurately. The dissolution of kaolinite led to the formation of sodalite ($Na_8Al_6Si_6O_{24}Cl_2$):

$$3Si_2Al_2O_5(OH)_4 + 8Na^+ + 2Cl^- + 6OH^- \rightarrow Na_8Al_6Si_6O_{24}Cl_2 + 9H_2O \quad (3)$$

The most disordered kaolinite samples were more difficult to dissolve and transform to sodalite (Table 1). The most ordered sample (kao-03) was completely dissolved by the end of the experiment with no obvious kaolinite peaks on the XRD pattern (Fig. 6a).

The following assignment of the FTIR bands of the original kaolinite samples (with the suffix 'before' in Fig 6b) was based on Farmer (1974). The band at 3620 cm^{-1} (ν_1) is from the stretching vibrations of inner OH groups, the bands at 3651 (ν_2), 3667 (ν_3), and 3688 (ν_4) cm^{-1} are from stretching vibrations of inner-surface OH groups. In agreement with the XRD patterns, the kaolinite peaks in the FTIR spectra decreased or disappeared after dissolution (suffix 'after' in Fig. 6b). The four OH-stretching bands were missing from the FTIR spectrum of kao-03 after the dissolution, two of the bands remained in kao-01 (ν_1 and ν_4), while the four bands remained in kao-05 except for a reduction in intensity. This corresponds to the complete dissolution of kaolinite in kao-03 (least disordered sample) and least dissolution in kao-05 (most disordered sample). The kaolinite bands at lower wavenumbers disappeared after dissolution to give rise to bands at 956–960, 730, 707, and 661 cm^{-1} which have been observed previously after the transformation of kaolin to sodalite (Li et al., 2015; Sari et al., 2018). Another observation in the OH-stretching region is the shift of ν_1 from 3688 cm^{-1} before the NaOH dissolution to 3696 cm^{-1} after NaOH dissolution, which was due to the matrix effect by sodalite. This matrix effect, observed in ATR mode, can be reproduced by artificially mixing kaolinite with pure sodalite (Fig. 7). When the kaolinite-sodalite mixture was washed with HCl to dissolve the sodalite, the in-phase OH band returned to 3688 cm^{-1} (Fig. 6c).

Intercalation of Kaolinite Residue after NaOH Dissolution

The SEM images of kao-01 after dissolution in NaOH (Fig. 8a) and after washing the kaolinite-sodalite matrix with HCl (Fig. 8b) indicated that the sodalite crystals formed in the former were fully dissolved by the acid wash. The kaolinite residue was characterized by jagged edges. The intercalant molecules could not surmount the interlayer binding strength of the kaolinite layers (despite observing the intercalation experiment for several weeks) (Fig. 9). The FTIR spectra of the kaolinite residue (Fig. 6c) registered similar band positions to those of the starting kaolinite except for the changes in the relative intensities of the OH bands. The intensities of ν_4/ν_1 and ν_2 were also reduced.

DISCUSSION

The kaolinite samples used in the present study were relatively pure with just traces of mica and anatase. The chemistry of the samples confirmed the ideal composition

https://doi.org/10.1007/s42860-021-00132-x Published online by Cambridge University Press

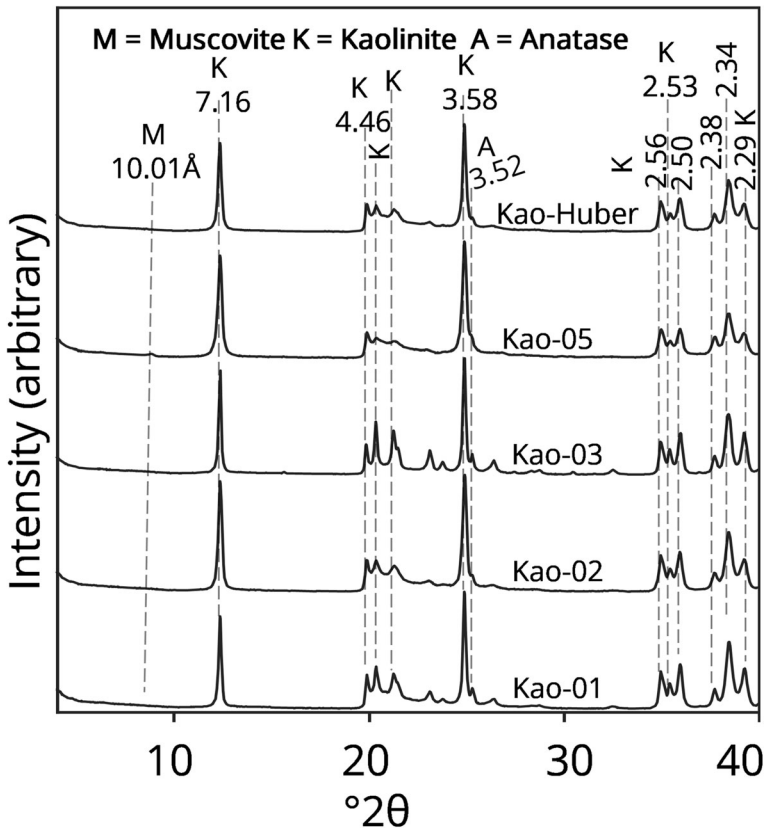


Fig. 3. XRD patterns of the 1–2 μm fraction of the kaolinites tested

($Al_2Si_2O_5(OH)_4$) and suggested little or no substitution of Fe for Al in the octahedral sheet. Such substitutions would have influenced the electrostatic energy and the degree of structural disorder of the mineral (Gaite et al., 1997; Iriarte et al., 2005) and consequently the reactivity. The influence of particles on the HI values and reactivity is also constrained given the similar particle-size distribution of the current kaolinite samples.

For intercalation to proceed, the intercalant molecules must first break the interlayer H-bond binding kaolinite layers. The ease of breaking this bond can be used as an indirect probe of the average interlayer binding strength. Going by the results of the first 4 h of intercalation (inset Fig. 5b), the disordered samples were more resistant to intercalation compared to ordered samples. The rate and degree of intercalation followed a similar trend to the degree of stacking order: kao-05 < kao-huber < kao-02 < kao-01 ≈ kao-03. Once the H-bonding between kaolinite layers is broken, intercalation proceeds. Yet, 100% intercalation is seldom observed, which can only mean that the H-bonding between some layers was not surmounted. This suggests that the interlayer binding strength is not uniform across layers. The results reported here suggest that disordered samples had greater average interlayer binding strength (i.e. stability) than the ordered samples. This conclusion contradicted Frost et al. (2002), who reported that the highly ordered Birdwood kaolinite intercalated very slowly

Table 1 The Hinckley Index (HI), the proportion of minerals, and the dissolution of the 1–2 μm fraction of five kaolinites

Specimen	HI	Crystallite Size* (nm)	Initial mineral compositions (%)			Dissolution in 4 M NaOH (%)
			Kaolinite	Mica	Anatase	
Kao-01	1.18	55–66	96.8	nd	3.2	86
Kao-02	0.94	49–52	97	nd	3	nt
Kao-03	1.50	61–71	97.5	nd	2.5	100
Kao-05	0.64	41–45	95.5	3.2	1.3	66
Kao-huber	0.87	48–53	98.3	nd	1.7	nt

*= along 00*l*; *nd* not detected, *nt* not tested

https://doi.org/10.1007/s42860-021-00132-x Published online by Cambridge University Press

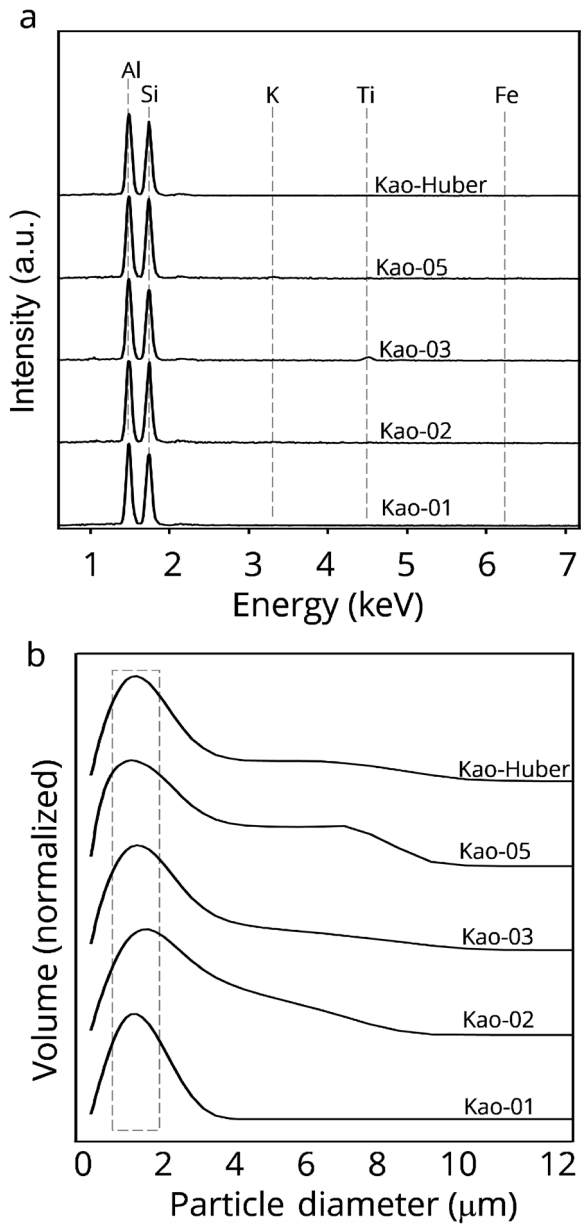


Fig. 4. **a** The EDS spectra and **b** normalized (volume = 0 to 1) particle-size distributions of the 1–2 μm kaolinite fractions

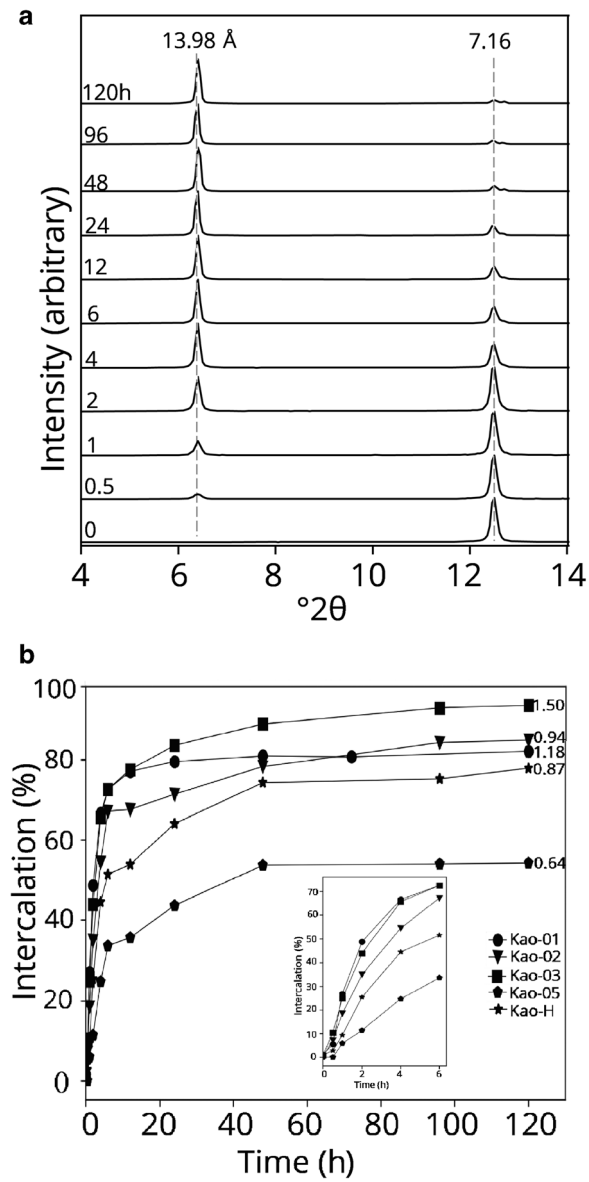


Fig. 5. Example of: **a** in situ XRD patterns of kao-03 during the intercalation experiment; and **b** percentages of intercalation of the 1–2 μm fractions of tested kaolinites

and to a lesser degree (20%) after 18 days. A likely reason for this exception is that Birdwood consisted mostly of small (0.5 μm) particles. Such very fine fractions have been well known not to intercalate easily. The pursuit of an explanation for this anomalous intercalation by very fine fractions has yielded several theories (Weiss et al., 1969; Wiewióra & Brindley, 1969; Raussell-Colom & Serratosa, 1987; Deng et al., 2002; Frost et al., 2002 Zhang & Xu, 2007).

The percent dissolution of kaolinite in 4 M NaOH followed a similar trend as the degree of structural disorder: kao-05 > kao-01 > kao-03. This result agreed with the intercalation experiment and suggested that highly disordered kaolinite had a greater binding strength than ordered kaolinite. The sharp, nearly symmetrically branched needle morphology of the residual kaolinite in the NaOH dissolution experiment suggested that only selected areas of the original kaolinite particle were dissolved by the NaOH (Fig. 8b). Under the experimental conditions used here, some layers within the highly disordered specimen were clearly more resistant to dissolution. The few available reports on structural order-dissolution relationships concluded mostly that disordered kaolinites were easier to dissolve compared to ordered specimens (Kittrick, 1966; Sutheimer et al., 1999). Hence, the current results contradicted these studies. An explanation is that in those studies, given that

https://doi.org/10.1007/s42860-021-00132-x Published online by Cambridge University Press

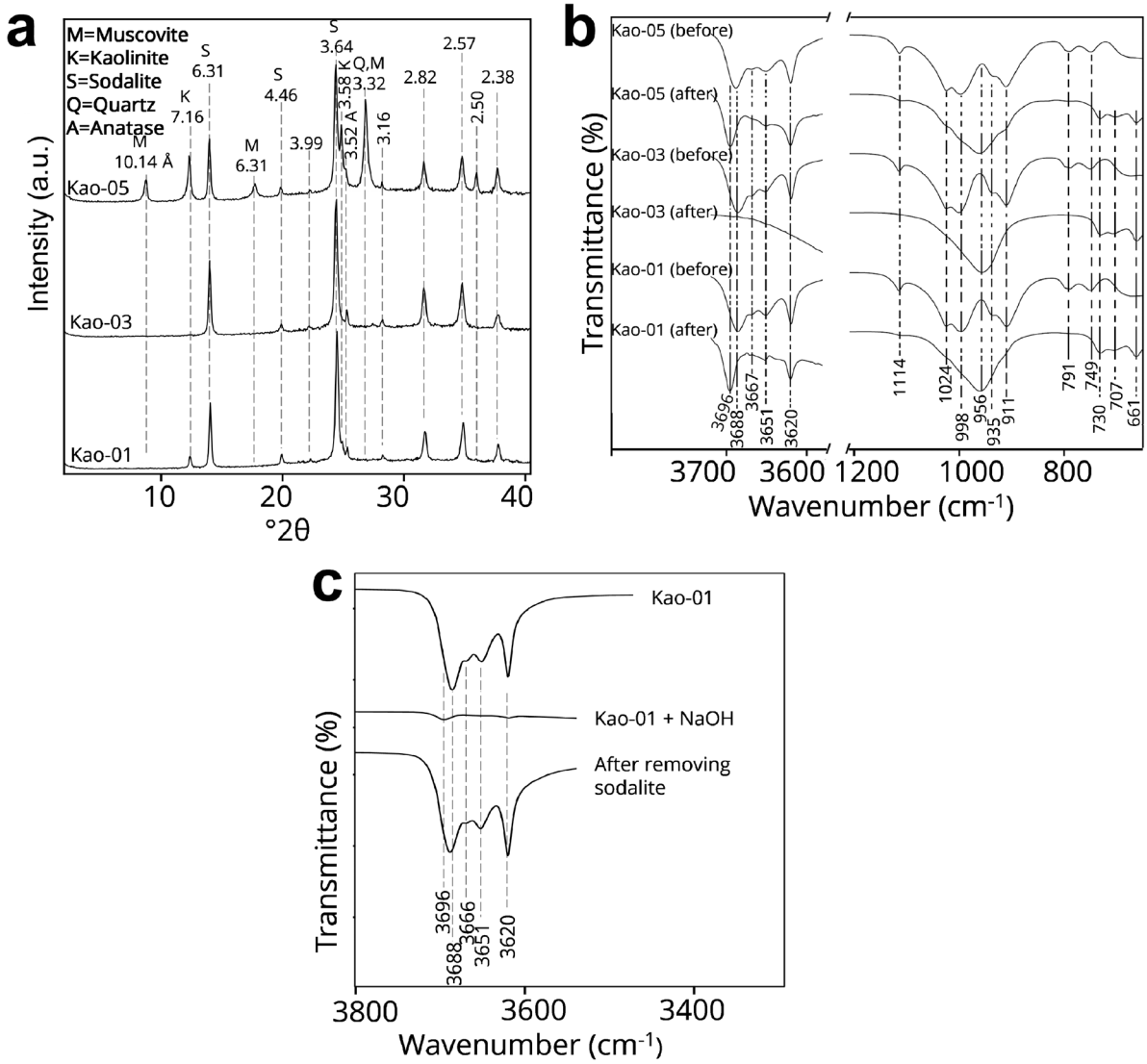


Fig. 6. a XRD patterns of the 1–2 μm fractions of kao-01, -03, and -05 after dissolution by 4 M NaOH; **b** FTIR spectra of the 1–2 μm fractions of kao-01, -03, and -05 before and after the dissolution by 4 M NaOH, and **c** FTIR spectra of kao-01 before (upper) and after (middle) dissolution in NaOH and after (lowest) washing in HCl. The 3700–3600 cm^{-1} section is magnified for clarity.

highly disordered samples were characterized by smaller particle sizes, the greater dissolution observed for disordered samples was more likely to be due to larger surface areas in the disordered specimens. When the different size fractions of kao-01 were dissolved in 4 M NaOH, the finer fractions showed more complete kaolinite dissolution (data not shown). By studying samples with a similar size distribution, the influence of size on dissolution was constrained.

Source of Differences in Interlayer Binding Strength

Having shown that the degree of structural disorder had a direct relationship with the reactivity, which, in turn, was related to the binding strength of kaolinite layers, a need remains to explain the sources of the observed differences in the binding strength of kaolinite of varying degrees of structural disorder. Though disorder due to the presence of stacking of enantiomorph layers $\boldsymbol{t_1t_2}$ is the most common type in kaolinite (Kogure et al., 2010; Kogure, 2011; Sakharov et al., 2016), these two types of displacements had little or no effect on the electrostatic energy of the system or on the hydrogen bonding between the layers because the C and C^e are identical layers that differ only in translation vector and are related by a pseudo-mirror plane passing through the center of the vacant octahedral site (Drits & Tchoubar, 1990; Giese, 1982). This also explains why the OH-stretching bands of several kaolinites are at almost the same frequencies, with only differences in relative intensity. Hence, the observed differences in reactivity/binding strength of kaolinite layers could not be explained by differences in the proportion of $\mathbf{t_1t_2}$ stacking disorder. On the

https://doi.org/10.1007/s42860-021-00132-x Published online by Cambridge University Press

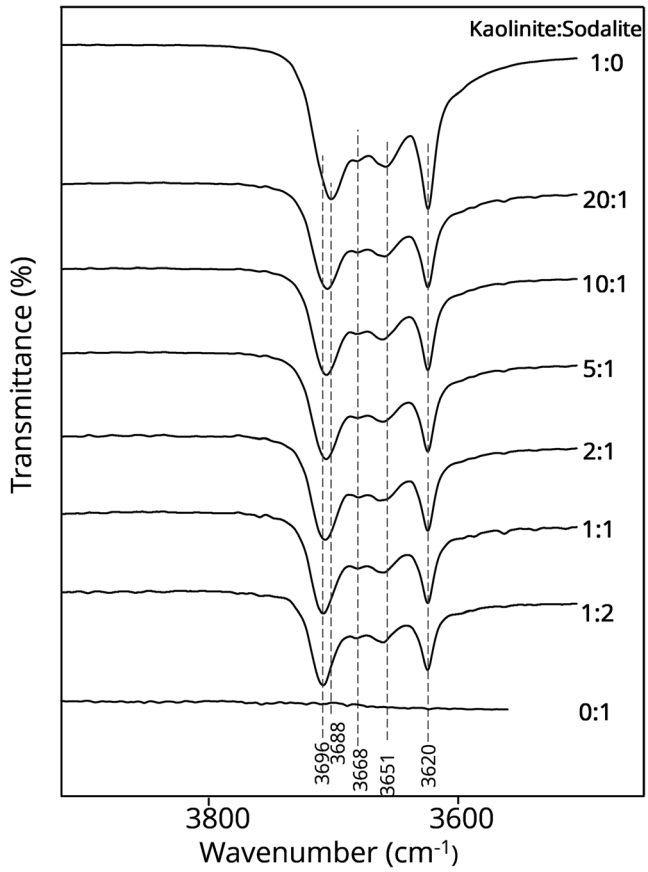


Fig. 7. Infrared (ATR) spectra of various ratios of kaolinite-sodalite mixture

other hand, dickite-like sequences (CB or BC) modify the relative position of the atoms located on both sides of the disordered layer (Drits & Tchoubar, 1990) and, as such, alter significantly the H-bonding between the layers. This form of stacking disorder is expected to influence the reactivity and stability of kaolinite layers.

Just as in the presence of a B-layer in the C-kaolinite, the $\mathbf{t_0}$ layer displacement leads to the creation of a new layer with atoms in a different position compared to $\mathbf{t_1}$ or $\mathbf{t_2}$ displacements and, thus, influences the binding strength of the layers. The insertion of $\mathbf{t_0}$ amongst $\mathbf{t_1}$ has the same effect on the calculated XRD patterns as inserting B-layers (Sakharov et al., 2016) and improves agreement between calculated and observed low-frequency regions (White et al., 2013).

Though the incorporation of dickite-like fragments or $\mathbf{t_0}$ displacements were expected to change the binding energetics of the layer in kaolinite, they have been shown to exist only in small percentages in sedimentary kaolinites (Plançon et al., 1989; Kogure & Inoue, 2005a; Kogure et al., 2010). The

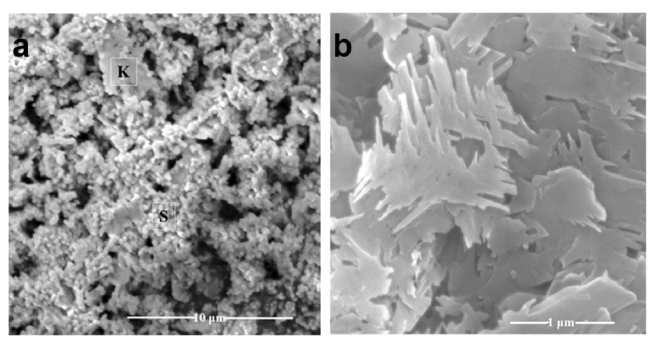


Fig. 8. SEM images of **a** sodalite (s, granular) precipitate and residual kaolinite (k, platy) in kao-01 after dissolution in 4 M NaOH and **b** the kaolinite residue after removing the sodalite with HCl

https://doi.org/10.1007/s42860-021-00132-x Published online by Cambridge University Press

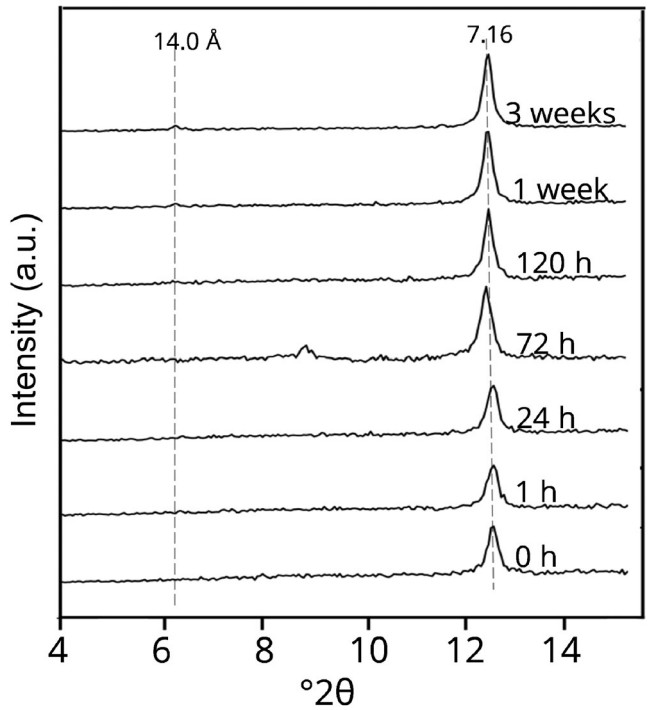


Fig. 9. In situ XRD patterns of the less reactive kaolinite residue of NaOH-reacted kao-01 during the intercalation experiment

dickite-like character is more common in hydrothermal kaolinites formed at relatively high temperatures (Kogure & Inoue, 2005b). By modeling XRD patterns, Sakharov et al. (2016) showed that the proportion of $\mathbf{t_0}$ displacements could not be great. A model containing 15–20% of $\mathbf{t_0}$ displacements resulted in calculated XRD patterns that deviated significantly from the experimental XRD patterns of KGa-1, KGa-1b, and KGa-2. The same authors also showed that the incorporation of 10% of B-layers led to a reduction in intensity and shifting of 131 reflections compared to the experimental pattern. Such shifts are observable in highly disordered kaolinite such as the Charente sedimentary kaolinite, however; this was shown to contain up to 15% of these layers (Drits & Tchoubar, 1990).

Thermodynamic and computational approaches have been used to investigate the stability of dickite and kaolinite layers, but the results are often contradictory. Using an electrostatic energy model, Giese (1973) showed computationally that the binding strength of dickite (CB) layers is 1.25 times greater than that of kaolinite (CC) layers while density functional state (DFT) calculations predicted a similar stacking energy for dickite or kaolinite layers (Sato et al., 2004). Thermodynamic approaches have shown that either dickite (Kiseleva et al., 2011; Zotov et al., 1998) or kaolinite is thermodynamically more stable (De Ligny & Navrotsky, 1999; Fialips et al., 2001, 2003). On the other hand, direct and simple experiments such as intercalation and dissolution appeared to suggest that dickite layers were more stable compared to kaolinite. For example, dickite layers were more difficult to intercalate than kaolinite (Cruz-Cumplido et al., 1982). Despite the size similarity of the kaolinite and dickite particles in Keokuk kaolinite, the kaolinite particles were shown (Fraser et al., 2002) to be more susceptible to dissolution by HF. Experimental results from dehydroxylation reactions, using infrared emission spectroscopy, showed that kaolinite lost inner-surface hydroxyls and inner hydroxyls simultaneously whereas dickite lost the inner surface hydroxyls before inner hydroxyls (Frost & Vassallo, 1996). This further suggests that the structure of dickite layers is more stable than that of kaolinite layers. Given that dickite-like sequences are also a source of disorder in kaolinites, the observed differences in reactivity as a function of stacking disorder could be explained at least partly. The failure of the kaolinite residue from the NaOH dissolution experiment to intercalate (Fig. 9) supports the view that the layer binding strength of the residual kaolinite was indeed greater than that of the dissolved ones. Compared to the starting material, the kaolinite residue appeared to exhibit more dickite-like character as shown by the decrease in the intensities of ν_1/ν_4 (1.185 to 0.969) band as ν_2 became slightly weaker, and the ν_2 band increased slightly by ~6% (Fig 6c). The distribution of the intensities of the OH-stretching bands in the residue was characteristic of FTIR patterns of dickite stacking containing kaolinite (Cuadros et al., 2015; Fraser et al., 2002; Prost et al., 1989). In synthetic mixtures of kaolinite and dickite, as the proportion of the latter increased, the ν_1/ν_4 ratio decreased and the ν_2 band became weaker. A shift in ν_1 to higher frequencies and the disappearance of ν_2 was also observed as the proportion of dickite became greater than 90% (Cuadros et al., 2015). Similar observations were made in the present study but no ν_1 shift was noted, suggesting that the less reactive residue still contained a significant proportion of kaolinite layers.

https://doi.org/10.1007/s42860-021-00132-x Published online by Cambridge University Press

Given the more dickite-like character of the residue, as observed in the IR spectrum, the present study concludes that the average layer binding strength of disordered kaolinites was greater than that of ordered kaolinites. One of the sources of this greater binding strength in disordered kaolinites is the presence of dickite-like stackings in disordered kaolinites.

CONCLUSIONS

The present study investigated the influence of structural disorder on the reactivity of kaolinites. To limit the contribution of particle size to the reactivity, only the 1–2 μm fraction of five kaolinites with similar particle-size distributions was used. Using saturated CH_3COOK solution as an intercalant and 4 M NaOH as a solvent, disordered kaolinites were more difficult to intercalate or dissolve compared to the more ordered kaolinites with very similar particle-size distributions. The kaolinite residue after 4 M NaOH dissolution was more difficult to intercalate than the starting kaolinite. Infrared data also suggested that the non-reactive portion in the NaOH dissolution contained more dickite-like features than the starting kaolinite. Having constrained the effect of the particle size on the reactivity of kaolinite, disordered kaolinites with a high degree of structural disorder had greater interlayer binding strength than the more ordered kaolinites. In addition to the common enantiomorphic stacking disorder, the former contains more dickite-like sequences in its stacking compared to the latter and contributed to the lower reactivity in the intercalation by CH_3COOK and dissolution by NaOH.

ACKNOWLEDGMENTS

The authors are grateful to the Norman Borlaug Institute, Texas A&M University, for the fellowship that sponsored the first author's graduate study, and the NSF grant DBI0116835 which supported the acquisition of the FE-SEM.

FUNDING

Funding sources are as stated in the Acknowledgments.

Declarations

Conflict of Interest

The authors declare that they have no conflict of interest.

REFERENCES

Beauvais, A., & Bertaux, J. (2002). In situ characterization and differentiation of kaolinites in lateritic weathering profiles using infrared microspectroscopy. *Clays and Clay Minerals, 50*, 314–330.

Bellotto, M., Gualtieri, A., Artioli, G., & Clark, S. M. (1995). Kinetic study of the kaolinite-mullite reaction sequence. Part I: Kaolinite dehydroxylation. *Physics and Chemistry of Minerals, 22*, 207–217.

Bish, D. L., & Von Dreele, R. B. (1989). Rietveld Refinement of Non-Hydrogen Atomic Positions in Kaolinite. *Clays and Clay Minerals, 37*(4), 289–296.

Bookin, A. S., Drits, V. A., Plançon, A., & Tchoubar, C. (1989). Stacking faults in kaolin-group minerals in the light of real structural features. *Clays and Clay Minerals, 37*, 297–307.

Brindley, G.W. (1980). Order-disorder in clay minerals. Pp. 125–196 in: *Crystal Structure of Clay Minerals and Their X-Ray Identification* (G.W. Brindley and G. Brown, editors). Mineralogical Society, London

Cheng, H., Liu, Q., Yang, J., Du, X., & Frost, R. L. (2010). Influencing factors on kaolinite–potassium acetate intercalation complexes. *Applied Clay Science, 50*, 476–480.

Cruz-Cumplido, M., Sow, C., & Fripiat, J. J. (1982). Spectre infrarouge des hydroxyles, cristallinité et énergie de cohésion des kaolins. *Bulletin de Minéralogie, 105*, 493–498.

Cuadros, J., Vega, R., & Toscano, A. (2015). Mid-infrared features of kaolinite-dickite. *Clays and Clay Minerals, 63*, 73–84.

De Ligny, D., & Navrotsky, A. (1999). Energetics of kaolin polymorphs. *American Mineralogist, 84*, 506–516.

Deng, Y., White, G. N., & Dixon, J. B. (2002). Effect of structural stress on the intercalation rate of kaolinite. *Journal of Colloid and Interface Science, 250*, 379–393.

Devidal, J. L., Dandurand, J. L., & Gout, R. (1996). Gibbs free energy of formation of kaolinite from solubility measurement in basic solution between 60 and 170°C. *Geochimica et Cosmochimica Acta, 60*, 553–564.

Drits, V.A. & Tchoubar, C. (1990). The modelization method in the determination of the structural characteristics of some layer silicates: Internal structure of the layers, nature and distribution of the stacking faults. Pp. 233–303 in: *X-Ray Diffraction by Disordered Lamellar Structures* (V.A. Drits and C. Tchoubar, editors). Springer, Berlin, Heidelberg.

Farmer, V. C. (1974). *The Infrared Spectra of Minerals*. Mineralogical Society of Great Britain and Ireland.

Fialips, C. I., Majzlan, J., Beaufort, D., & Navrotsky, A. (2003). New thermochemical evidence on the stability of dickite vs. kaolinite. *American Mineralogist, 88*, 837–845.

Fialips, C. I., Navrotsky, A., & Petit, S. (2001). Crystal properties and energetics of synthetic kaolinite. *American Mineralogist, 86*, 304–311.

Franco, F., Pérez-Maqueda, L. A., & Pérez-Rodríguez, J. L. (2003). The influence of ultrasound on the thermal behaviour of a well ordered kaolinite. *Thermochimica Acta, 404*, 71–79.

Fraser, A. R., Wilson, M. J., Roe, M. J., & Shen, Z. Y. (2002). Use of hydrofluoric acid dissolution for the concentration of dickite and nacrite from kaolin deposits: an FTIR study. *Clay Minerals, 37*, 559–570.

Frost, R. L., Kristof, J., Horvath, E., & Kloprogge, J. T. (1999). Modification of kaolinite surfaces through intercalation with potassium acetate, II. *Journal of Colloid and Interface Science, 214*, 109–117.

Frost, R. L., Van Der Gaast, S. J., Zbik, M., Kloprogge, J. T., & Paroz, G. N. (2002). Birdwood kaolinite: a highly ordered kaolinite that is difficult to intercalate—an XRD, SEM and Raman spectroscopic study. *Applied Clay Science, 20*, 177–187.

Frost, R. L., & Vassallo, A. M. (1996). The dehydroxylation of the kaolinite clay minerals using infrared emission spectroscopy. *Clays and Clay Minerals, 44*, 635–651.

Gaite, J. M., Ermakoff, P., Allard, T., & Muller, J. P. (1997). Paramagnetic Fe^{3+}: A sensitive probe for disorder in kaolinite. *Clays and Clay Minerals, 45*, 496–505.

Galán, E., Aparicio, P., La Iglesia, Á., & Gonzalez, I. (2006). The effect of pressure on order/disorder in kaolinite under wet and dry conditions. *Clays and Clay Minerals, 54*, 230–239.

Giese, R. F. (1973). Interlayer bonding in kaolinite, dickite and nacrite. *Clays and Clay Minerals, 21*, 145–149.

Giese, R. F. (1982). Theoretical-studies of the kaolin minerals-electrostatic calculations. *Bulletin de Minéralogie, 105*, 417–424.

Giese, R.F. (1988). Kaolin Minerals: Structures and Stabilities. Pp. 29–66 in: *Hydrous Phyllosilicates (Exclusive of Micas)* (S.W. Bailey, editor). Reviews in Mineralogy, *19*. Mineralogical Society of America, Chantilly, Virginia, USA.

Hinckley, D. N. (1962). Variability and "crystallinity" values among the koalin deposits of the coastal plain of Georgia and South Carolina. *Clays and Clay Minerals, 11*, 229–235.

https://doi.org/10.1007/s42860-021-00132-x Published online by Cambridge University Press

Horváth, I. (1985). Kinetics and compensation effect in kaolinite dehydroxylation. *Thermochimica Acta, 85*, 193–198.
Iriarte, I., Petit, S., Huertas, F. J., Fiore, S., Grauby, O., Decarreau, A., & Linares, J. (2005). Synthesis of kaolinite with a high level of Fe^{3+} for A1 substitution. *Clays and Clay Minerals, 53*, 1–10.
Johnston, C. T., Elzea-Kogel, J., Bish, D. L., Kogure, T., & Murray, H. H. (2008). Low-temperature FTIR Study of Kaolin-Group Minerals. *Clays and Clay Minerals, 56*, 470–485.
Kiseleva, I. A., Orogodova, L. P., Krupskaya, V. V., Melchakova, L. V., Vigasina, M. F., & Luse, I. (2011). Thermodynamics of the kaolinite-group minerals. *Geochemistry International, 49*, 793–801.
Kittrick, J. A. (1966). Free energy of formation of kaolinite from solubility measurements. *American Mineralogist, 51*, 1457–1466.
Kogure, T. (2011). Stacking disorder in kaolinite revealed by HRTEM: A review. *Clay Science, 15*, 3–11.
Kogure, T., Elzea-Kogel, J., Johnston, C. T., & Bish, D. L. (2010). Stacking disorder in a sedimentary kaolinite. *Clays and Clay Minerals, 58*, 62–71.
Kogure, T., & Inoue, A. (2005a). Determination of defect structures in kaolin minerals by high-resolution transmission electron microscopy (HRTEM). *American Mineralogist, 90*, 85–89.
Kogure, T., & Inoue, A. (2005b). Stacking defects and long-period polytypes in kaolin minerals from a hydrothermal deposit. *European Journal of Mineralogy, 17*, 465–474.
Kristof, E., Juhasz, A. Z., & Vassanyi, I. (1993). The effect of mechanical treatment on the crystal structure and thermal behavior of kaolinite. *Clays and Clay Minerals, 41*, 608–612.
Li, J., Zeng, X., Yang, X., Wang, C., & Luo, X. (2015). Synthesis of pure sodalite with wool ball morphology from alkali fusion kaolin. *Materials Letters, 161*, 157–159.
Liétard, O. (1977). *Contribution a l'etude des proprietes physicochimiques, cristallographiques et morphologiques des kaolins [thesis]*. University of Nancy.
Lombardi, G., Russell, J. D., & Keller, W. D. (1987). Compositional and structural variations in the size fractions of a sedimentary and a hydrothermal kaolin. *Clays and Clay Minerals, 35*, 321–335.
Mahdavi, F., Abdul, R. S., & Khanif, Y. M. (2014). Intercalation of urea into kaolinite for preparation of controlled release fertilizer. *Chemical Industry and Chemical Engineering Quarterly, 20*, 207–213.
Momma, K., & Izumi, F. (2011). VESTA 3 for three-dimensional visualization of crystal, volumetric and morphology data. *Journal of Applied Crystallography, 44*, 1272–1276.
Panagiotopoulou, C., Kontori, E., Perraki, T., & Kakali, G. (2007). Dissolution of aluminosilicate minerals and by-products in alkaline media. *Journal of Materials Science, 42*, 2967–2973.
Plançon, A., Giese Jr., R. F., Snyder, R., Drits, V. A., & Bookin, A. S. (1989). Stacking faults in the kaolin-group minerals: Defect structures of kaolinite. *Clays and Clay Minerals, 37*, 203–210.
Prost, R., Dameme, A., Huard, E., Driard, J., & Leydecker, J. P. (1989). Infrared study of structural OH in kaolinite, dickite, nacrite, and poorly crystalline kaolinite at 5 to 600 K. *Clays and Clay Minerals, 37*, 464–468.
Raussell-Colom, J.A. & Serratosa, J.M. (1987). Chemistry of clays and clay minerals. Pp. 371–422 in: *Chemistry of Clays and Clay Minerals* (A.C. Newman, editor). Monograph **6**, Mineralogical Society of Great Britain & Ireland, London.
Reyes, C. A. R., Williams, C., & Alarcón, O. M. C. (2013). Nucleation and growth process of sodalite and cancrinite from kaolinite-rich clay under low-temperature hydrothermal conditions. *Materials Research, 16*, 424–438.
Rietveld, H. M. (1967). Line profiles of neutron powder-diffraction peaks for structure refinement. *Acta Crystallographica, 22*, 151–152.
Sakharov, B. A., Drits, V. A., McCarty, D. K., & Walker, G. M. (2016). Modeling powder X-ray diffraction patterns of The Clay Minerals Society kaolinite standards: KGa-1, KGa-1b, and KGa-2. *Clays and Clay Minerals, 64*, 314–333.
Sari, M. E. F., Suprapto, S., & Prasetyoko, D. (2018). Direct synthesis of sodalite from kaolin: the influence of alkalinity. *Indonesian Journal of Chemistry, 18*, 607.
Sato, H., Ono, K., Johnston, C. T., & Yamagishi, A. (2004). First-principle study of polytype structures of 1:1 dioctahedral phyllosilicates. *American Mineralogist, 89*, 1581–1585.
Scherrer, P. (1918). Estimation of the size and internal structure of colloidal particles by means of Röntgen. *Nachrichten von der Gesellschaft der Wissenschaften zu Göttingen, 2*, 96–100.
Soukup, D.A., Buck, B.J., & Harris, W. (2008). Preparing soils for mineralogical analyses. Pp. 13–31 in: *Methods of Soil Analysis Part 5—Mineralogical Methods*. SSSA Book Series SV - 5.5, Soil Science Society of America, Madison, WI, USA.
Stoch, L., & Wacławska, I. (1981). Dehydroxylation of kaolinite group minerals - I. Kinetics of dehydroxylation of kaolinite and halloysite. *Journal of Thermal Analysis, 20*, 291–304.
Sugahara, Y., Nagayama, T., Kuroda, K., Dio, A., & Kata, C. (1991). Preparation of a kaolinite-acrylic acid intercalation compound and the heat-treated products. *Clay Science, 8*, 69–77.
Sutheimer, S. H., Maurice, P. A., & Zhou, Q. (1999). Dissolution of well and poorly crystallized kaolinites: Al speciation and effects of surface characteristics. *American Mineralogist, 84*, 620–628.
Theng, B.K.G. (editor) (1974). *The Chemistry of Clay–Organic Reactions*. Wiley and Sons, New York, London 343 pp.
Uwins, P.J.R., Mackinnon, I.D.R., & Thompson, J.G. (1991). "Crystallinity" and intercalation relationships in size fractionated Australian kaolinites. P. 154 in: *Clay Minerals Society 28th Annual Meeting*.
Uwins, P. J. R., Mackinnon, I. D. R., Thompson, J. G., & Yago, A. J. E. (1993). Kaolinite-NMF intercalates. *Clays and Clay Minerals, 41*, 707–717.
Vaculikova, L., Plevova, E., Vallova, S., & Koutnik, I. (2011). Characterization and differentiation of kaolinites from selected Czech deposits using infrared spectroscopy and differential thermal analysis. *Acta Geodynamica et Geromaterialia, 8*, 59–68.
Veblen, D. R. (1985). Direct TEM imaging of complex structures and defects in silicates. *Annual Review Earth and Planetary Sciences, 13*, 119–146.
Weiss, A., Becker, H.O., Orth, H., Mai, G., Lechner, H., & Range, K.J. (1969). Particle size effects and reaction mechanism of the intercalation into kaolinite. Pp. 180–184 in: *Proceedings of the International Clay Conference, Tokyo*.
White, C. E., Kearley, G. J., Provis, J. L., & Riley, D. P. (2013). Structure of kaolinite and influence of stacking faults: Reconciling theory and experiment using inelastic neutron scattering analysis. *Journal of Chemical Physics, 138*, 194501.
White, N.G. & Dixon, J.B. (2002). Kaolin-serpentine minerals. Pp. 389–414 in: *Soil Mineralogy with Environmental Applications* (J.B. Dixon and D.G. Schulze, editors). Soil Science Society of America, Madison, WI, USA.
Wiewióra, A. & Brindley, G.W. (1969). Potassium acetate intercalation in kaolinite and its removal; effect of material characteristics. Pp. 723–733 in: *Proceedings of the International Clay Conference 1969, Tokyo*.
Xu, B., Smith, P., Wingate, C., & De Silva, L. (2010). The effect of calcium and temperature on the transformation of sodalite to cancrinite in Bayer digestion. *Hydrometallurgy, 105*, 75–81.
Zhang, X. R., & Xu, Z. (2007). The effect of microwave on preparation of kaolinite/dimethylsulfoxide composite during intercalation process. *Materials Letters, 61*, 1478–1482.
Zhao, H., Deng, Y., Harsh, J. B., Flury, M., & Boyle, J. S. (2004). Alteration of kaolinite to cancrinite and sodalite by simulated hanford tank waste and its impact on cesium retention. *Clays and Clay Minerals, 52*, 1–13.
Zotov, A., Mukhamet-Galeev, A., & Schott, J. (1998). An experimental study of kaolinite and dickite relative stability at 150–300°C and the thermodynamic properties of dickite. *American Mineralogist, 83*, 516–524.

(Received 5 August 2020; revised 22 April 2021; AE: Giorgios D. Chryssikos)

https://doi.org/10.1007/s42860-021-00132-x Published online by Cambridge University Press